JOURNAL OF MATERIALS SCIENCE 29 (1994) 5719–5724

Processing characteristics of Al/W composite under 1 *g* conditions

S. C. SHARMA, P. R. NARAYANAN, P. P. SINHA, K. V. NAGARAJAN
Materials and Metallurgy Group, Vikram Sarabhai Space Centre, Trivandrum 695 022, India

The segregation features and interface characteristics in an Al/W composite system processed through liquid metallurgy technique under 1 *g* conditions has been studied. The effect of various melting parameters on the Al/W system containing 60 wt% (about 20 at%) tungsten particles, was investigated and the consequent metallographic features of these composites were studied. Although most of the segregation of tungsten particles was observed at the bottom of the sample, segregation was also noticed towards the side walls and the top portion of the sample. The segregation pattern is explained in terms of force under Stoke's law and conventional convection. The formation of intermetallic compounds between aluminium and tungsten, and limited solubility between these two elements, is also reported.

1. Introduction

The microgravity environment of space offers very conducive terms for processing composite materials through the liquid metallurgy (LM) route, because the effects due to gravity-driven phenomena (e.g. buoyancy and density and temperature-based convection) are considerably minimized. Quite a few experiments [1–14] have been carried out under microgravity environment to process the metal matrix-based composites by the LM technique. These experiments were designed to study either the individual or the combined effect of buoyancy, convection and particle–front interactions in the solidifying composite melts. The results of these experiments generally reveal that it is possible to achieve improved uniformity of dispersion in the reduced gravity environment. They also show that surface tension force, which remains masked under Earth-bound conditions, becomes dominant in space, and it causes segregation in composite melts owing to surface-tension driven convection [5, 14].

The microgravity environment of space is not completely free from buoyancy effects. The various residual external forces, e.g. atmospheric drag and solar radiation pressure, transient external forces (e.g. thruster firings for attitude control and other orbital manoeuvres) acting around the spacecraft and internal forces (called *g*-jitters, due to the motion of mechanical parts, crew activities, etc.), acting inside the spacecraft, result in accelerations ranging from 10^{-3}–10^{-7} *g* [15, 16]. The buoyancy force, because of these accelerations, can cause segregation in the composite melt even if it is processed on board a spacecraft. The segregation will be more pronounced if the difference between the densities of matrix and dispersoid is significantly large. In most of the experiments conducted so far, this difference has not been very large and, therefore, they do not reveal any such effect. The present work was undertaken mainly to study the influence of residual acceleration and *g*-jitter driven buoyancy force on the uniformity of the distribution of dispersoids in the matrix. The Al/W composite system was selected because the density difference between aluminium and tungsten represents a nearly extreme situation and, therefore, the influence can be studied more clearly. However, in the absence of any literature on the processing of Al/W composites, it is necessary to observe the processing characteristics of this system first on Earth (1 *g*) itself. The scope of the present paper is confined to the results of experiments carried out to process Al/W composites via the LM route under 1 *g* conditions. Our studies mainly comprise observations with respect to (i) segregation features, and (ii) interface characteristics, in the above-processed Al/W system.

2. Experimental procedure

The samples were prepared by the powder metallurgy technique. The matrix metal and second-phase particles of aluminium and tungsten, respectively, were of 99.9% purity. About 60 wt % W powder (3–7 μm) was thoroughly mixed with the aluminium powder (8–40 μm) on a roller mixer. Being of very high density, 60 wt % tungsten powder in an Al/W system is equivalent to only about 20 at % tungsten powder. Tungsten powder was treated in a hydrogen atmosphere at 700 °C for 2 h prior to its mixing with aluminium powder. Compacts of 13.5 mm × 11.0 mm × 6.0 mm size were made by cold pressing the mixed powder under a pressure of 35 kg mm^{-2}. The compacts were heated in alumina crucibles for melting under an extensive flow of argon gas in a precision tubular furnace. The argon gas before entering the furnace, was passed through a purification apparatus consisting of pyrogallic acid and dried α-alumina to remove traces of oxygen and moisture. The details of the melting parameters and corresponding sample

0022–2461

TABLE I Summary of melting conditions

Serial no.	Melting parameters		Sample designation
	Temperature (°C)	Duration of soaking (min)	
1	670	50	I
2	750	40	II
3	950	30	III

designations are given in Table I. All samples after melting were cooled in air.

The samples were subjected to conventional polishing and etched with Keller's Reagent to enable various metallographic examinations to be made. The microstructures were observed using a Reichert MEF2 optical microscope (OM), and a Leitz miniload microhardness tester was used for microhardness measurements on various phases. The samples were further studied under higher resolution in a scanning electron microscope (SEM, Cambridge Stereoscan 250 Mk III), with 20 kV, 3 A as operating parameters. The identification of various phases was done by the X-ray diffraction (XRD) method, using a Phillips system with 35 kV and 20 mA as operating parameters. The elemental composition of various phases was determined using energy dispersion analysis of X-rays (EDAX, Tracor Northern Inc., USA).

3. Results and discussion

The macroscopic polished and etched surface of the green compact and a similar surface of the cross-section of Sample III are given in Fig. 1. Figs 2–4 represent optical and scanning electron micrographs at various locations in the green compact and Samples I and III. Table II contains the microhardness data. The results of the semi-quantitative analysis carried out through EDAX at various locations in the samples, are given in Table III, while Fig. 5 shows the EDAX profiles at the areas depleted and segregated with tungsten particles in Sample III. Fig. 6 exhibits X-ray diffraction profiles for Samples I and III.

As is evident from the SEM observations in Fig. 2, tungsten particles (bright phase) are uniformly distributed in the aluminium powder matrix in the green compact. However, tungsten particles, being much smaller than aluminium particles, are preferentially located in the inter-particle region of aluminium particles and form a well-connected network all over the matrix. Porosity is also present all along the network of tungsten particles.

The interesting visual observation about Sample I was that although it contracted noticeably after heating at 670 °C for 50 min, its rectangular shape was not disturbed. Microstructures of Sample I (Fig. 3) denote a situation wherein the melting of aluminium powder matrix has just begun. The distinct well-connected network of tungsten powder which was present in the green compact is broken and these powder particles are now comparatively more intimately mixed with the aluminium matrix (Fig. 3a and b). The distribution of tungsten particles in the aluminium matrix is still intact. EDAX analysis (Table III) reveals that some tungsten particles which were earlier located in the inter-particle region of aluminium particles in the green compact, have now migrated to the melted aluminium areas, but alumi-

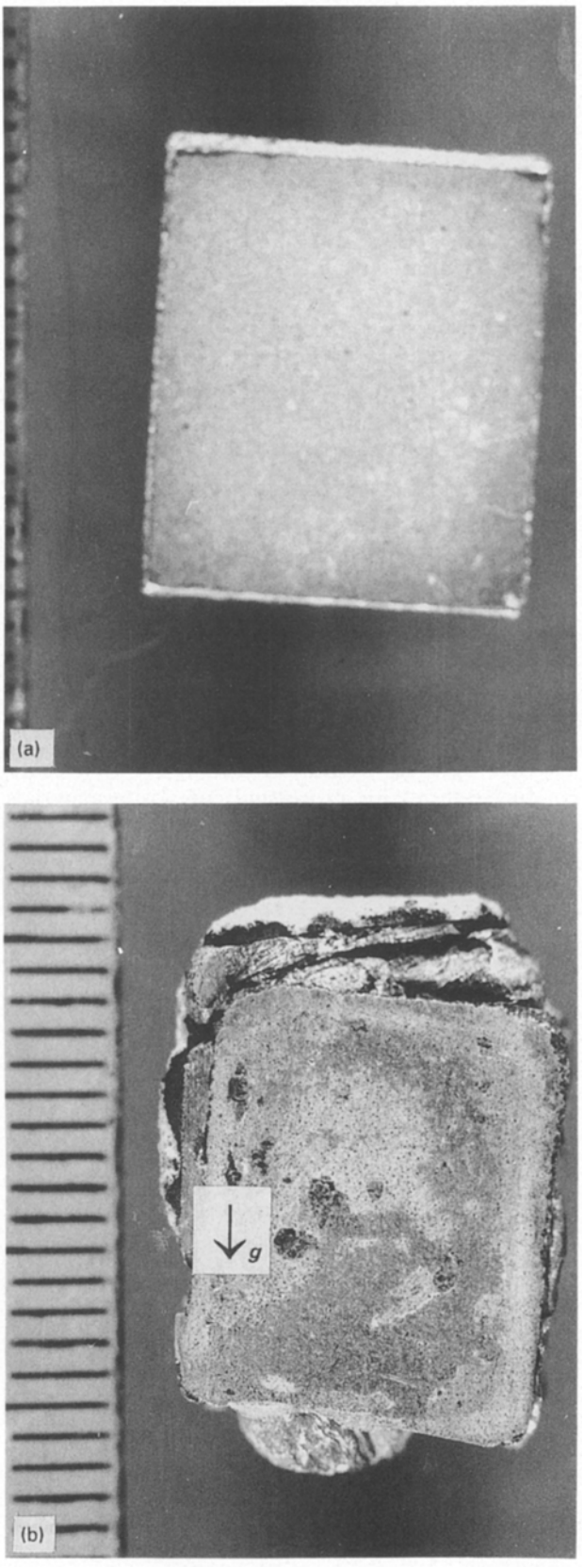

Figure 1 Macroscopic polished and etched surface of (a) green compact, and (b) a cross-section of Sample III.

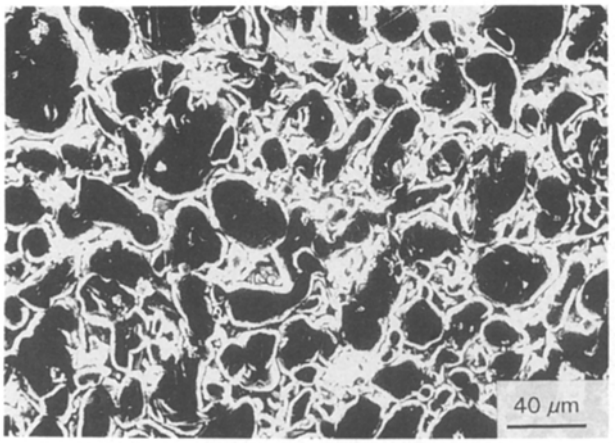

Figure 2 Scanning electron micrograph of the green compact.

nium-rich and tungsten-rich areas still mark the distribution pattern all over the matrix. There is no indication of any gravity-driven segregation. This can be attributed to the existence of only partial remelting conditions in Sample I. In a similar partial remelting experiment on the Al/SiC composite system, Bayoumi and Suery did not note any segregation owing to gravity [17].

A scanning electron micrograph of Sample I at larger magnification (Fig. 3c) shows that porosity is still present. The XRD profile (Fig. 6a) on Sample I, in addition to indicating aluminium and tungsten in elemental form, shows the presence of intermetallic phase WAl_{12}. The WAl_{12} phase, with 36.23 wt % (7.69 at %) W and b c c crystal structure, is reported to form by the peritectic reaction, liquid + $WAl_5 \rightleftharpoons WAl_{12}$ at 697 °C [18].

Therefore, WAl_{12} must have formed in the tungsten-rich areas in the sample. The microhardness values (Table II) in Sample I are higher than those in the green compact. This is an indication of the improved interface characteristics between the aluminium matrix and tungsten particles. The observations in Sample II were not much different from Sample I. Hence, further discussion is based on the observations made from Samples I and III only.

Although considerable contraction was observed in Sample III when it was taken out of the furnace after heating at 950 °C for 30 min, the rectangular shape of the sample was also not disturbed in this case. However, when the sample was mildly pressed with the tongs immediately after its being taken out of the furnace, the liquid metal squeezed out (Fig. 1b). The possible formation of a very thin aluminium oxide layer or skin all around the sample during heating at elevated temperature, must have prevented the flow of liquid metal which was very small in volume (0.891 cm^3). Froyen and Deruyttere, who performed a series of experiments on the LM processing of the small samples of Al/SiC composites under 1 g and microgravity conditions, have also reported the containment of melt by the Al_2O_3 skin [19].

As shown in Figs 1b and 4, there is large segregation of tungsten particles at the bottom of Sample III. Some segregation, though remarkably less compared to the bottom, can also be observed towards the

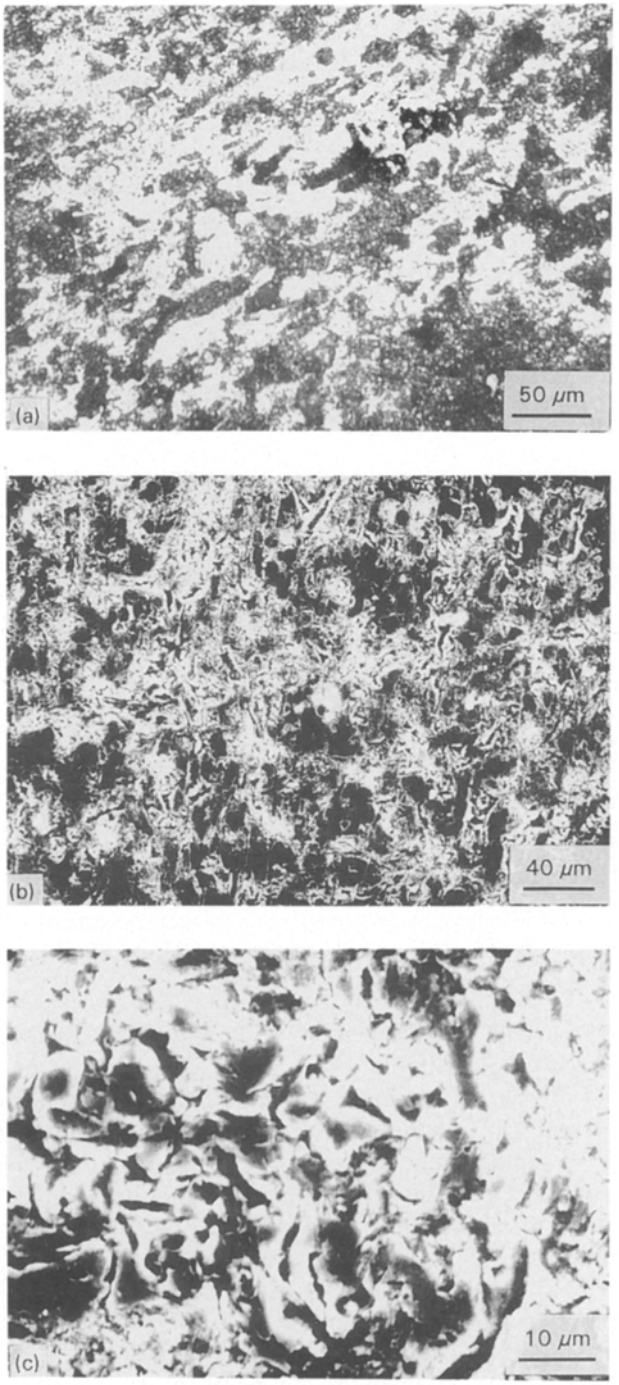

Figure 3 Metallographic observations on Sample I through (a) OM, (b) SEM, and (c) at higher resolution in SEM.

vertical sides and the upper portion of the sample. The large-scale depletion of tungsten particles from the core of the sample and their segregation at the bottom, sides and top, are supported by the EDAX spectra in Fig. 5. The large segregation at the bottom has occurred mainly due to gravity-driven sedimentation. The effectiveness of the sedimentation force can be estimated by Stoke's law, in terms of terminal velocity, V_t, of the settling tungsten particles (assumed spherical). According to this law

$$V_t = \frac{d^2 g \Delta\rho}{18 \eta} \quad (1)$$

where d is the diameter of a particle, g the acceleration due to gravity, $\Delta\rho$ the difference between the density of

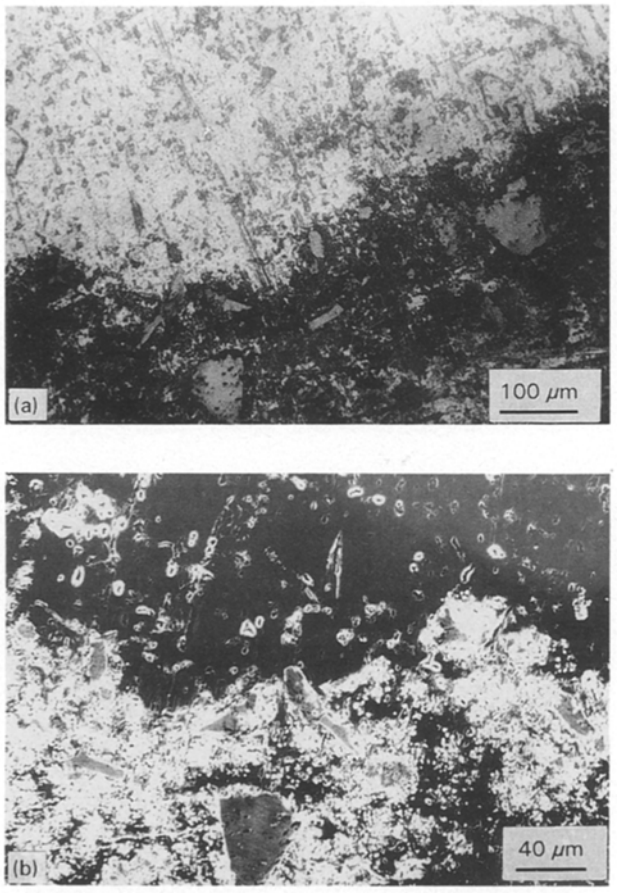

Figure 4 Metallographic observations on the area segregated with tungsten particles in Sample III, through (a) OM, and (b) SEM.

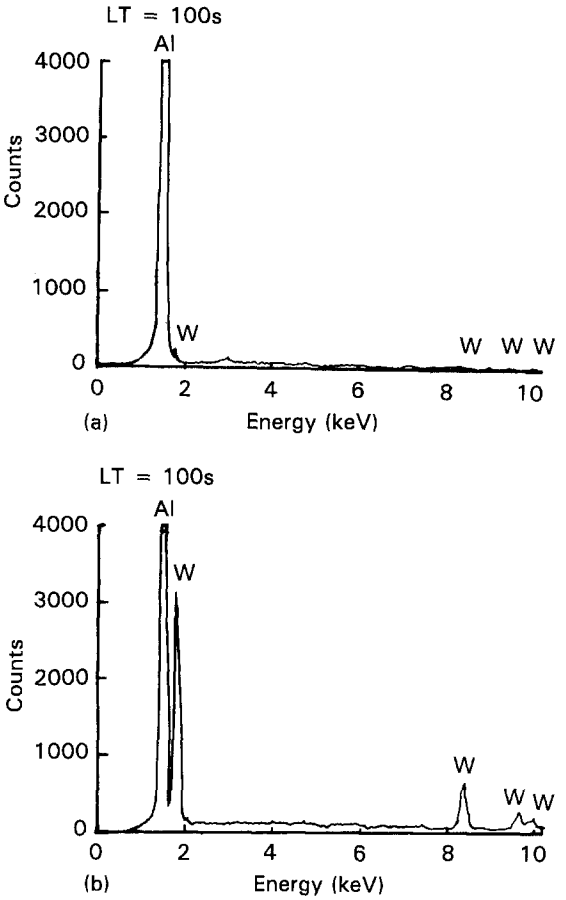

Figure 5 Energy dispersive spectra of Sample III: (a) area depleted of tungsten particles, and (b) area segregated with tungsten particles. Elemental analysis: (a) Al, 99.31 wt %, 99.88 at %; W, 0.35 wt %, 0.05 at %; (b) Al, 45.82 wt %, 84.86 at %; W, 53.51 wt %, 14.54 at %.

the particle and the density of the liquid, and η the viscocity of the liquid.

For the calculation of terminal velocities in the present Al/W system, the following data are used: $d = 5\ \mu m$ (average diameter of tungsten particles), $g = 9.8\ m\ s^{-2}$, $\Delta\rho = 16\,886\ kg\ m^{-3}$ (density of tungsten $= 19\,254\ kg\ m^{-3}$ and density of liquid aluminium at $950\,^{\circ}C = 2368\ kg\ m^{-3}$ [20]), and $\eta = 2.1 \times 10^{-3}$ Pas (liquid viscocity of aluminium [21]). With tungsten particles of 5 μm, V_t is in the proximity of 6.9 mm min^{-1} under terrestrial conditions. Under residual accelerations of the order of $10^{-3}\ g$, this velocity is as low as 0.69×10^{-2} mm min^{-1}. For a tungsten particle of 100 μm, $V_t = 2.74 \times 10^2$ mm min^{-1} and 0.27 mm min^{-1} on Earth and under $10^{-3}\ g$, respectively.

As regards the segregation of tungsten particles along the vertical sides and towards the top of the sample, similar observations were reported by Froyen and Deruyttere in their experiment on LM processing of Al/SiC composite systems under 1 g conditions [19]. They attributed this to the conventional convection caused by a temperature gradient. The fluid flow under the influence of convection is characterized by a flow velocity that is determined by the Grashof number (Gr). Froyen and Deruyttere show that even a small radial temperature difference (0.1 K) can cause considerable flow (0.6 mm s^{-1}) at the normal gravity level in Al/SiC systems. A temperature gradient in the longitudinal direction can cause thermally unstable convection if the Rayleigh number, Ra (Ra = PrGr, where Pr is the Prandtl number) exceeds a critical value. Corresponding to the critical Ra value of 10^6 for their sample, they computed a critical temperature gradient (dT/dl) of $12 \times 10^3\ K\ m^{-1}$ under 1 g.

Our experiment differs from that of Froyen and Deruyttere in the choice of dispersoid. Froyen and Deruyttere chose SiC particles of 125–160 μm diameter. The temperature gradient in the aluminium melt in Sample II in our experiment can be set by the settling tungsten particles under Stoke's law, because the thermal properties of aluminium and tungsten differ significantly. However, under no probability, the temperature gradient can reach the critical value of 12

TABLE II Microhardness data

Serial no.	Sample	Location	Vickers Hardness (H_V) Load 50 g
1	Green compact	Bright phase Dark phase	32–34 51–54
2	Sample I	Matrix + dispersoid	55–68
3	Sample III	Area depleted with tungsten particles	35–49
		Area segregated with tungsten particles	90–101

TABLE III EDAX Analysis of various samples

Serial no.	Sample	Region	Element	(at %)	(wt %)
1	Green compact	Bright phase (Al-rich area)	Al	98.56	91.73
			W	1.24	7.88
		Dark phase (W-rich area)	Al	23.88	4.40
			W	76.12	95.60
2	Sample I	Al-rich area	Al	97.73	86.65
			W	2.18	13.18
		W-rich area	Al	80.02	37.07
			W	19.91	62.85
3	Sample III	Area depleted with tungsten particles	Al	99.88	99.51
			W	0.05	0.35
		Area segregated with tungsten particles	Al	84.86	45.82
			W	14.54	53.51

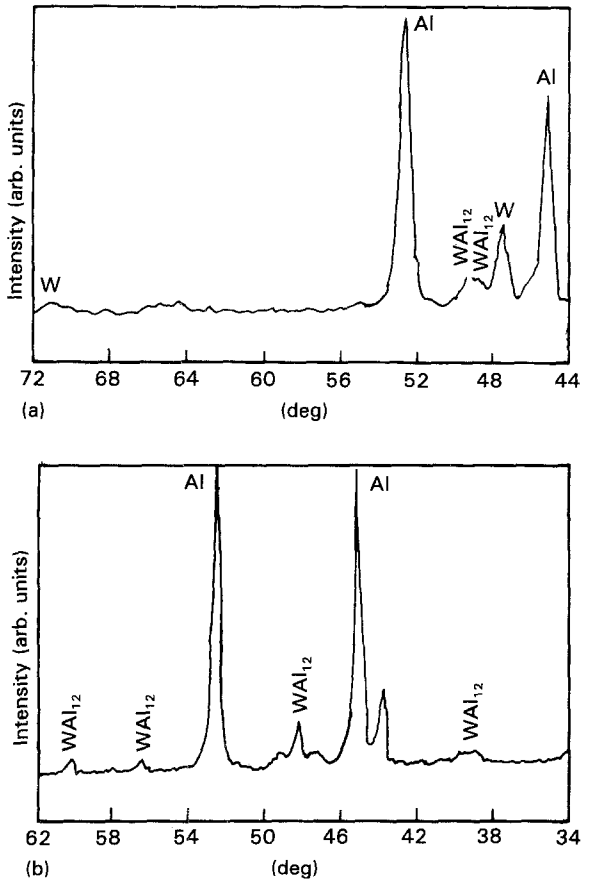

Figure 6 XRD profiles on (a) Sample I, and (b) Sample III.

$\times 10^3$ K m^{-1} and, therefore, conditions for unstable or turbulent convection are ruled out. The convection flow at the dT/dl levels below a critical limit is laminar [22] and transportation of the particles from the central part to the side walls too can be assigned to this laminar flow. However, the presence of convection currents in the melt will affect, though not very greatly, the terminal velocity of the settling particles.

Fig. 4 suggests that Sample III is free from porosity. The microhardness of the tungsten-segregated areas in Sample III (Table II) is significantly higher than that in tungsten-rich areas in the green compact. This can be attributed to the stronger interfaces between tungsten particles and the aluminium matrix in the segregated areas consequent to the melting of the matrix. The molten state of the matrix encourages chemical interaction between the particles and the matrix. In addition to the presence of aluminium and tungsten in elemental form and intermetallic compounds (Fig. 6b) in the segregated areas, the XRD data also indicate the formation of a solid solution between aluminium and tungsten. This was determined by calculating the variation in the lattice parameter of the aluminium lattice which forms the matrix. This is achieved by fitting a curve for $\cos^2\theta$ versus a_0 based on the regression analysis of the XRD data. As calculated using this method, the lattice parameters for the aluminium matrix in Samples I and III are 0.405 379 and 0.405 347 nm, respectively, while the standard lattice parameter of aluminium is 0.404 910 nm [18]. The change in the lattice parameter of aluminium with the addition of tungsten is an indication of solid solubility between aluminium and tungsten which is also reported elsewhere [18, 23].

4. Conclusions

1. The segregation in the Al/W composite processed through the LM technique is mainly caused by sedimentation (buoyancy) force and conventional convection.

2. The interface characteristics are improved, subsequent to the melting of the aluminium matrix because of the chemical interactions between the tungsten particles and the matrix.

3. Very limited solid solubility between aluminium and tungsten and the formation of intermetallic compounds between tungsten and aluminium are observed.

4. The sedimentation (buoyancy) effects due to residual accelerations in the microgravity environment of space will be better revealed by a tungsten particle of 100 μm diameter in the aluminium matrix.

Acknowledgements

The authors thank Shri. D. Easwaradas, Deputy Director, VSSC (MMS), for his support of this programme, and also Mr P. S. Rao and other colleagues

of the Metallography and Heat-treatment sections of MMG for their assistance. Permission was granted by the Director, VSSC, to publish this paper, and is gratefully acknowledged.

References

1. L. CASTELLANI, P. GONDI, F. BARBIERI and N. COSTA, in "Proceedings of the 3rd European Symposium on Material Sciences in Space", Grenoble, 1979, edited by T. D. Guyenne (ESA Scientific and Technical Publications Branch, Noordwijk) ESA SP-142, p. 81.
2. D. UHLMAN, NASA Report TM-X 3458 (NASA) Ch. III, pp. III. I–III. 40.
3. D. M. STEFANESCU, A. MOITRA, A. S. KACAR and B. K. DHINDAW, *Met. Trans.* **21A** (1990) 231.
4. B. K. DHINDAW, A. MOITRA, D. M. STEFANESCU and P. CURRERI, *ibid.* **19A** (1988) 1899.
5. J. POTSCHKE and K. HOHENSTEIN, *Acta Astronaut.* **9** (1982) 261.
6. F. BARBEIRI, C. PATUELLI, P. GONDI and R. MONTANARI, in "Proceedings of the 5th European Symposium on Materials Sciences under Microgravity", Schloss Elmau, 1984, edited by T. D. Guyenne, ESA SP-222, p. 101.
7. H. KLEIN and R. NAHLE, in "Proceedings of the 4th European Symposium on Materials Sciences under Microgravity", Madrid, 1983, edited by T. D. Guyenne and J. Hunt,. ESA SP-191, p. 37.
8. T. KAWADA, S. YOSHIDA, S. YAKAHASHI, E. OZAGA and R. YODA, in "AIAA 15th Aerospace Meeting", (1977), p. 77.
9. S. TAKAHASHI, in "Proceedings of the 5th International Conference on Composite Materials", San Diego, CA, (1985) p. 747.
10. R. J. NAUMANN and H. W. HERRING, "Materials Processing in Space: Early Experiments" (NASA Scientific and Technical Information Branch, Washington, 1980), p. 70.
11. D. R. UHLMANN, SPAR V Final Report, NASA TM 78275 (NASA, 1980), pp. II.1–II.49.
12. *Idem*, SPAR IV Final Report, NASA T M 78235 (NASA, 1980), pp. II.1–II.46.
13. L. RAYMOND and C. Y. ANG, SPAR II Final Report, NASA TM-X 78–215 (NASA) p. II.1
14. H. U. WALTER, in "Proceedings of the 3rd European Symposium on Materials Sciences in Space", p. 245.
15. H. HAMACHER, in "Materials Sciences in Space", edited by B. Feuerbacher, H. Hamacher and R. J. Naumann (Springer, 1986) p. 34.
16. V. S. AVDUYEVSKY, (ed.), "Scientific Foundations of Space Manufacturing" (MIR, Moscow, 1984) p. 32.
17. M. A. BAYOUMI and M. SUERY, in "Proceedings of the World Materials Congress", edited by Fishwan and Dhingra (ASM, Chicago, 1988), p. 167.
18. L. F. MONDOLFO, "Aluminium Alloys: Structures and Properties" (Butterworths, London, 1976) p. 394.
19. L. FROYEN and A. DERUYTTERE, in "Proceedings of the 5th European Symposium on Materials Sciences under Microgravity", p. 69.
20. "Metals Handbook", Vol. 2 10th Edn, (ASM International, 1990) p. 1090.
21. A. MOITRA, B. K. DHINDAW and D. M. STEFANESCU, in "Proceedings of the Conference on Solidification of Metal Matrix Composites", Indianapolis, edited by P. Rohatgi (TM, PA, 1990) p. 159.
22. S. RAMSESHAN, in "Proceedings of the Workshop on Materials Processing in Space", Bangalore, edited by S. Ramseshan and M. K. Tiwari (Indian Academy of Sciences, Bangalore, 1982) p. 3.
23. RODNEY P. ELLIOTT, "Constitution of Binary Alloys" (McGraw-Hill, New York, 1965) p. 63.

Received 18 March 1993
and accepted 6 January 1994.